Phase-sensitive reflection of squeezed vacuum field in optical cavity

Ke Di (邸　克), Xudong Yu (于旭东), Fengyu Cheng (程峰钰), and Jing Zhang (张　靖)*

State Key Laboratory of Quantum Optics and Quantum Optics Devices, Institute of Opto-Electronics,

Shanxi University, Taiyuan 030006, China

*Corresponding author: jzhang74@sxu.edu.cn; jzhang74@yahoo.com

We experimentally investigate the optical cavity for various coupled regimes with an injected squeezed vacuum state. We measure the quantum fluctuation spectra of the reflected field of an optical cavity using the homodyne detection and present the spectral dependence on the absorption and dispersion properties of the cavity in the under-coupled, critically-coupled, and over-coupled regimes. The spectra lineshape is phase sensitive with the phase shift induced by the cavity. Moreover, we find that the over-coupled optical cavity has obvious advantage in the manipulation of quantum fluctuation.

OCIS codes: 190.4360, 230.1150, 270.1670.

doi: 10.3788/COL201210.091901.

The optical cavity has a wide range of applications in scientific and commercial instruments, such as laser, spectroscopy, frequency stabilization, etc. An important property of optical cavity is its dispersive and absorptive response. A cavity can be over-coupled, critically-coupled (impedance matched)[1], or under-coupled. The phase of the field reflected from the cavity is also important for frequency lock acquisition[2−4] and optical pulse transmission. More specifically, on-resonance, over-coupled cavity results in slow light, whereas under-coupled cavity results in fast light, and critically-coupled cavity results in zero reflection[5−7].

The quantum noise of light can be manipulated by employing the optical cavity. Quantum sidebands of bright light beam are modified by the optical cavity, in which original quantum phase fluctuations of the incident bright beam are converted into amplitude fluctuations[3,8−13] (note that only amplitude fluctuations of bright light beam can be detected directly by the photodiode). The tomography of quantum states of bright light beam can be performed using this method[10,11]. The quantum fluctuation spectra of the subharmonic reflected field of a degenerate optical parametric amplifier (OPA) inside an optical cavity have been studied theoretically[14] and experimentally[15], which is driven by the squeezed vacuum state. The quantum fluctuation spectra for an optical empty cavity and the two-coupled cavities with an injected squeezed vacuum state have also been investigated in Refs. [15] and [16]. In these works, only over-coupled cavity is considered since its phase response undergoes a 2π phase shift. In this letter, we experimentally study the quantum fluctuation spectra of the reflected field from an optical cavity with various coupled regimes when injecting the squeezed vacuum state systematically. The squeezed quadrature components of the reflected beam of the optical cavity are measured by choosing the phase of the local beam relative to the input squeezed vacuum state. We demonstrate how the absorption and dispersion properties of the cavity determine the quantum fluctuation spectra of the reflected field. To the best of our knowledge, this work is completely different from the most previous studies for bright light injecting an optical cavity[3,8−13].

An optical cavity is assumed to be a standing wave cavity with the length L and comprises of input mirror M_1 and back mirror M_2. The round trip time of the cavity is $\tau = 2L/c$. The light resonates in the optical cavity and reflects from M_1. The motion equation for the intracavity light field is expressed as

$$\tau\frac{d\hat{a}}{dt} = -i\Delta\tau\hat{a} - \gamma\hat{a} + \sqrt{2\gamma_{in}^a}\hat{a}_{in} + \sqrt{2\rho}\hat{a}_v, \qquad (1)$$

where γ is the total damping of the cavity expressed by $\gamma = \gamma_{in}^a + \rho$, γ_{in}^a is the damping associated with input mirror M_1, ρ is the decay rate for internal losses, Δ is the detuning between the cavity-resonance frequency and the seed light frequency with $\Delta = 4\pi(L - L_{res})/\tau\lambda = \nu_c - \nu_L$, where λ is the wavelength of the light, L_{res} is the cavity length at resonance, ν_c is cavity resonant frequency, and ν_L is the frequency of injecting light. Furthermore, $\hat{a}_v$ is the vacuum noise which is coupled into the cavity through internal losses.

First, we consider that the bright light field is injected into the optical cavity, which may be expressed as $\hat{a}_{in} = a_{in} + \delta\hat{a}_{in}$, where a_{in} is the mean field of the bright light, and $\delta\hat{a}_{in}$ is quantum fluctuation. Without loss of generality, we assume that the phase of the injected bright light field is zero, i.e, a_{in} is real and positive. The steady state solution corresponding to $d\hat{a}/dt = 0$ in Eq. (1) is given by

$$0 = -i\Delta\tau a - \gamma a + \sqrt{2\gamma_{in}^a}a_{in}. \qquad (2)$$

Combining the boundary condition $a_o = a_{in} - \sqrt{2\gamma_{in}^a}a$, we could get the steady state solutions of the reflected field of the optical cavity as

$$a_o = -\frac{2\gamma_{in} - \gamma - i\Delta\tau}{\gamma + i\Delta\tau}a_{in}. \qquad (3)$$

The mean values of the reflected field a_o may be expressed as $a_o = |a_o|\exp(i\theta)$. The amplitude $|a_o|$ and

phase θ of the reflected field with respect to the detuning Δ may be plotted by Eq. (3) as shown in Fig. 1. Note that Eq. (3) gives the lineshape of amplitude and phase shift only near zero detuning within one free spectral range (FSR). However, the method in Refs. [5–7] may gives the lineshape for any frequency detuning (for example, the periodic structure when the frequency range exceeds one FSR). Figures 1(a) and (d) show the lineshape of amplitude and phase shift with respect to the detuning Δ for the under-coupled cavity ($\gamma_{in}^a < \rho$). Near resonance, the amplitude presents the loss and the phase undergoes a rapid variation with respect to the detuning. For an undercoupled cavity, the phase is a dispersion-shaped response that never exceeds $\pm\pi/2$. The derivative $d\theta/d\Delta$ of the phase is analogous to group refractive indices. According to the lineshape of phase shift with respect to the detuning, the under-coupled cavity results in fast light at resonance and may generate slow light at out of resonance. When the optical cavity becomes a critically-coupled cavity ($\gamma_{in}^a = \rho$, also called impedance-matched cavity), the resulting amplitude and phase shift curves are shown in Figs. 1(b) and (e). The amplitude of the reflected field is zero at resonance. When $\gamma_{in}^a > \rho$, the cavity is overcoupled. The phase responde undergoes a 2π phase shift when the cavity goes through resonance, as shown in Fig. 1(f), which corresponds to slow light. When the cavity is changed from overcoupled regime (undercoupled) to critically-coupled configuration, the group velocity becomes increasingly slower (faster).

Now, let us consider the situation only with the input quantum field ($\hat{a}_{in} = \delta\hat{a}_{in}$, and $a_{in} = 0$). The conjugate of Eq. (3) can be obtained as

$$\tau\frac{d\hat{a}^\dagger}{dt} = i\Delta\tau\hat{a}^\dagger - \gamma\hat{a}^\dagger + \sqrt{2\gamma_{in}^a}\hat{a}_{in}^\dagger + \sqrt{2\rho}\hat{a}_v^\dagger. \quad (4)$$

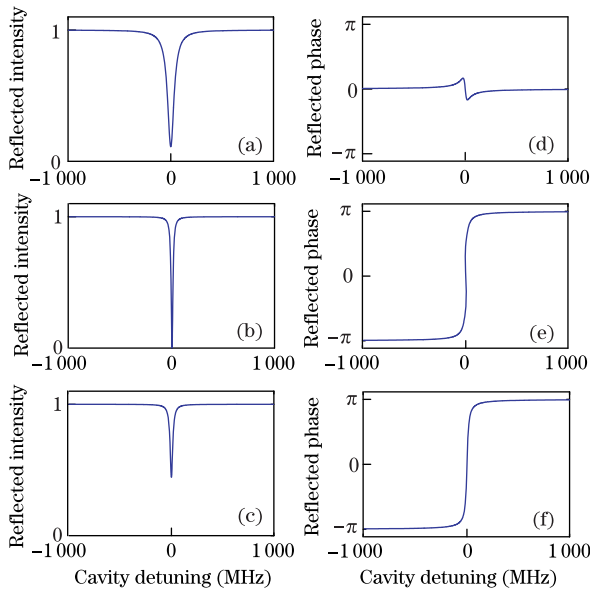Since the spectra of the quadrature variances of the

Fig. 1. (Color online). Lineshape of amplitude and phase of the reflected coherent light from the cavity as a function of the cavity detuning. (a) and (d) with the under-coupled optical cavity ($\gamma_{in}^a = 0.05$ and $\rho = 0.1$); (b) and (e) with critically-coupled optical cavity ($\gamma_{in}^a = 0.05$ and $\rho = 0.05$); (c) and (f) with over-coupled optical cavity ($\gamma_{in}^a = 0.05$ and $\rho = 0.01$).

reflection field are measured and analyzed by homodyne detection, we make the Fourier transformation $\delta\hat{a}(\omega) = \frac{1}{\sqrt{2\pi}}\int dt\delta\hat{a}(t)e^{-i\omega t}$. We could obtain

$$\delta\hat{a}(\omega) = \frac{2\sqrt{\gamma_{in}^a}\delta\hat{a}_{in}(\omega) + 2\sqrt{\rho}\delta\hat{a}_v(\omega)}{\gamma + i(\omega + \Delta)\tau}, \quad (5)$$

$$\delta\hat{a}^\dagger(-\omega) = \frac{2\sqrt{\gamma_{in}^a}\delta\hat{a}_{in}^\dagger(-\omega) + 2\sqrt{\rho}\delta\hat{a}_v^\dagger(-\omega)}{\gamma + i(\omega - \Delta)\tau}. \quad (6)$$

According to the boundary condition $\delta\hat{a}_o = \delta\hat{a}_{in} - \sqrt{2\gamma_{in}^a}\delta\hat{a}_{in}$, the amplitude and phase quadratures of the reflected field are expressed by

$$\delta\hat{X}_a = \delta\hat{a}(\omega) + \delta\hat{a}^\dagger(-\omega), \quad (7)$$

$$\delta\hat{Y}_a = -i[\delta\hat{a}(\omega) + \delta\hat{a}^\dagger(-\omega)]. \quad (8)$$

We can get the amplitude and phase quadratures of the reflected field as

$$\delta\hat{X}_o = \{[2\gamma_{in}^a\gamma - \gamma^2 - (\Delta^2 - \omega^2)\tau^2 + 2i\omega\tau(\gamma_{in}^a - \gamma)]\delta\hat{X}_{in}$$
$$+ 2\gamma_{in}^a\Delta\tau\delta\hat{Y}_{in} + 2\sqrt{\gamma_{in}^a}\rho(\gamma + i\omega\tau)\delta\hat{X}_v$$
$$- 2\sqrt{\gamma_{in}^a}\rho\Delta\tau\delta\hat{X}_v\}/[\gamma^2 + (\Delta^2 - \omega^2)\tau^2 + 2i\omega\tau\gamma], \quad (9)$$

$$\delta\hat{Y}_o = \{[2\gamma_{in}^a\gamma - \gamma^2 - (\Delta^2 - \omega^2)\tau^2 + 2i\omega\tau(\gamma_{in}^a - \gamma)]\delta\hat{Y}_{in}$$
$$- 2\gamma_{in}^a\Delta\tau\delta\hat{X}_{in} + 2\sqrt{\gamma_{in}^a}\rho(\gamma + i\omega\tau)\delta\hat{Y}_v$$
$$+ 2\sqrt{\gamma_{in}^a}\rho\Delta\tau\delta\hat{Y}_v\}/[\gamma^2 + (\Delta^2 - \omega^2)\tau^2 + 2i\omega\tau\gamma]. \quad (10)$$

Thus, we can get the fluctuation variances of the amplitude and phase quadratures of the reflected field from the optical cavity

$$\langle\delta^2\hat{X}_o\rangle = [(2\gamma_{in}^a\gamma - \gamma^2 - \Delta^2\tau^2 + \omega^2\tau^2)^2\langle\delta^2\hat{X}_{in}\rangle$$
$$+ 4\omega^2\tau^2(\gamma_{in}^a - \gamma)^2\langle\delta^2\hat{X}_{in}\rangle + 4(\gamma_{in}^a\Delta\tau)^2\langle\delta^2\hat{Y}_{in}\rangle$$
$$+ 4\gamma_{in}^a\rho(\gamma^2 + \omega^2\tau^2)\langle\delta^2\hat{X}_v\rangle + 4\gamma_{in}^a\rho\Delta^2\tau^2\langle\delta^2\hat{Y}_v\rangle]$$
$$/[(\gamma^2 + \Delta^2\tau^2 - \omega^2\tau^2)^2 + 4\omega^2\tau^2\gamma^2], \quad (11)$$

$$\langle\delta^2\hat{Y}_o\rangle = [(2\gamma_{in}^a\Delta\tau)^2\langle\delta^2 X_{in}\rangle + 4\gamma_{in}^a\rho\Delta^2\tau^2\langle\delta^2\hat{X}_v\rangle$$
$$+ (2\gamma_{in}^a\gamma - \gamma^2 - \Delta^2\tau^2 + \omega^2\tau^2)^2\langle\delta^2\hat{Y}_{in}\rangle$$
$$+ 4\omega^2\tau^2(\gamma_{in}^a - \gamma)^2\langle\delta^2\hat{Y}_{in}\rangle$$
$$+ 4\gamma_{in}^a\rho(\gamma^2 + \omega^2\tau^2)\langle\delta^2\hat{Y}_v\rangle]$$
$$/[(\gamma^2 + \Delta^2\tau^2 - \omega^2\tau^2)^2 + 4\omega^2\tau^2\gamma^2]. \quad (12)$$

The experimental setup is shown in Fig. 2. The light source is a diode-pumped intracavity frequency-doubled continuous-wave ring Nd:YVO$_4$/KTP laser, which simultaneously provides about 200 mW of the green light at 532 nm and 50 mW of the fundamental light at 1 064 nm. The green light is injected into the optical parametric oscillator (OPO) as a pump beam. The fundamental light, after tranforming into cleaning mode by passing through the mode clean cavity, is divided into two parts: one part is used as local oscillator (LO) for the balanced homodyne detector, and another beam is used as the signal beam to be injected into the OPO. The output fundamental beam for the OPO is then injected into the optical empty cavity. This signal beam is mainly utilized for alignment of OPO and the optical empty cavity, because the squeezed
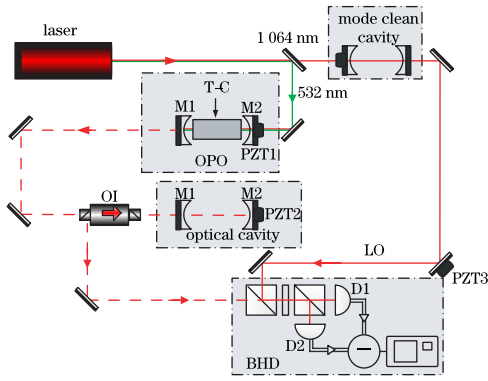
Fig. 2. (Color online) Schematic of the experimental setup for the manipulation of a squeezed vacuum field by an optical empty cavity. A squeezed vacuum state is generated from the subthreshold OPO and then injected into the optical empty cavity. DC: dichroic mirror; T-C: temperature controller; PBS: polarizing beam splitter; OI: optical isolator; D1 and D2: detectors; BHD: balance homodyne detection.

vacuum state has very low numbers of photon and is very difficult to align. The OPO cavity and the optical empty cavity have the same structures, each of which is composed of two mirrors with the same radius of curvature of 30 mm. Inside the OPO cavity, there is a 12-mm-long periodically poled KTP (PPKTP) crystal mounted in a copper block, which is connected with temperature control unit that could control the temperature of crystal at the millidegree Kelvin level around the operation temperature (31.3 °C) for optimizing the optical parametric down-conversion process at the chosen wavelength. For the OPO cavity, mirror M1 has a reflectivity of 88.7% at 1 064 nm and is a high reflector (> 99%) at 532 nm as well as the reflectivity of mirror M2 99.5% at 1 064 nm and 30% at 532 nm. The pump light is injected into the OPO through mirror M2, and the output of squeezed vacuum light generated from the OPO is at mirror M1. For the optical empty cavity, input mirror M1 has a reflectivity of 95.8% at 1 064 nm, but the reflectivity of mirror M2 is variational. The two mirrors are separated by ∼59 mm. Mirror M2 is mounted on a PZT2 in order to adjust the length of cavity. According to the reflectivity of M2, we can classify the optical empty cavity into under-coupled (90%), critically-coupled (95%), or over-coupled cavity (99.2%).

When blocking the signal fundamental light and opening the pump light for the OPO, the output squeezed vacuum light is injected into the optical empty cavity at mirror M1 through the optical isolator, which could separate the reflected beam from the optical empty cavity. The reflected beam is combined with the LO field at a 50/50 beam splitter, and then detected by the balanced homodyne detector (BHD) system. The relative phase between the LO field and the squeezed vacuum field reflected from M1 of the optical empty cavity is adjusted by the PZT3. The interference efficiency of homodyne detection system may reach 94.5% in the experiment by optimizing the mode-matching between LO and the reflected signal light. The squeezed vacuum light at the sideband frequency of 2.5 MHz is analyzed and recorded by RF spectrum analyzer.

First, when we block mirror M2 of the optical empty cavity and choose the relative phase between the LO

field and the squeezed vacuum field, we could obtain the quantum fluctuations of the OPO without the influence of the optical empty cavity. As shown in Fig. 3(a), the spectrum (blue curve) is below the shot-noise limit (SNL) (black curve) when we fix the relative phase between LO and the reflected signal light to be $\phi = 0$, which corresponds to measuring the squeezing component. Since $\phi = \pi/2$, as we can see in Fig. 3(b), the spectrum (blue curve) of the antisqueezing component is far above the SNL. The squeezing with 1.7 dB and antisqueezing component with 6 dB are detected by the BHD system.

Now, let us turn on the optical empty cavity and scan its length by PZT2. Choosing the reflectivity of M2 of the optical empty cavity, we can obtain the quantum fluctuation of the reflected field of an under-coupled cavity, a critically-coupled cavity, and an over-coupled cavity.

Case 1. We first study the spectra of the reflected squeezed vacuum field from the under-coupled optical cavity with respect to the cavity detuning, as shown in Figs. 3(c) and (d). Fixing the relative phase between LO and the reflected signal light to be $\phi = 0$, the squeezing quadrature of the reflected field is measured (Fig. 3(c)). Near resonance, the measured quadrature component, becomes $\delta \hat{X}^\theta = \cos\theta \hat{X} + \sin\theta \hat{Y}$, where θ is the phase
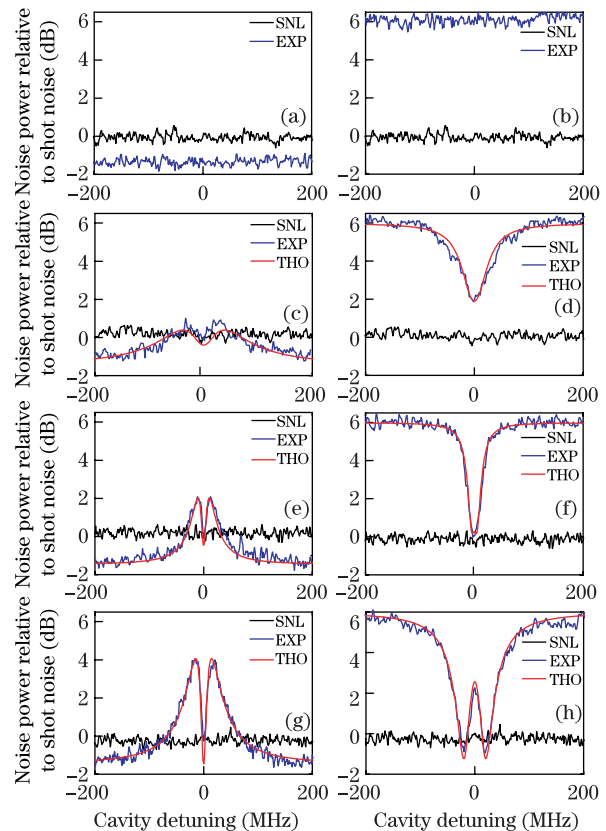

Fig. 3. (Color online) Reflection spectra of the squeezed and antisqueezed components from the optical cavity injected with the squeezed vacuum field as a function of the cavity detuning. (a) and (b) Without the optical cavity; (c) and (d) with the under-coupled optical cavity; (e) and (f) with the critically-coupled optical cavity; (g) and (h) with the over-coupled optical cavity. The blue curves are the experimental results, and the red curves are the theoretical calculations.

shift of the cavity (thus, the antisqueezing component can be measured at the detuning with $\theta = \pi/2$ induced by the cavity, which is above the SNL). Because of the absorption and dispersion properties of the optical cavity, the reflected spectrum of squeezed quadrature presents M-type profile. At zero detuning, the degree of the squeezing can still be slightly measured due to zero phase shift induced by the cavity, however it is decreased due to the cavity loss. Thus, the spectrum at the center is below the SNL, although, the squeezing is smaller than that at far off resonance. In comparision, the squeezing at far off resonance corresponds to nearly prefect reflection. When choosing the relative phase between the LO and squeezed vacuum field to be $\phi = \pi/2$, the antisqueezing quadrature component of the reflected field is shown in Fig. 3(d). The reflected spectrum of antisqueezed quadrature presents a dip at the center.

Case 2. Let us investigate the situation with the optical empty cavity near critically-coupled configuration. When we fix the relative phase to be $\phi = 0$, two shoulders of the reflected spectrum at close resonance (Fig. 3(e)) are higher than that of case 1, since there is larger phase shift θ induced by the cavity as shown in Fig. 1(e). When the relative phase is set as $\phi = \pi/2$, the reflected spectrum of the antisqueezing component (Fig. 3(f)) is shown as the V profile, in which the dip in the center is deeper than that of case 1. This is because the amplitude of the reflected field is zero at resonance for the critically-coupled cavity, as shown in Fig. 1(b).

Case 3. Now we concentrate on the quantum fluctuation reflected from over-coupled optical cavity injected with the squeezed vacuum light, as shown in Figs. 3(g) and (h). With the measurement of the squeezed component, the lineshape of the reflected spectrum from the over-coupled optical cavity still maintains the M profile, but the shoulders become higher than those in cases 1 and 2 and may reach the level of the input antisqueezing component, which is due to the lower loss and larger phase shift for the over-coupled cavity. There is a phase shift $\theta = \pi/2$ induced by the cavity at the two shoulders. The degree of the squeezing at zero detuning is below the SNL and reaches the degree of the input squeezing for the strongly over-coupled cavity. With the measurement of the antisqueezed component, the noise spectrum presents a W profile, as shown in Fig. 3(h). The noise level at zero detuning reaches the level of the input antisqueezing component for the strongly over-coupled cavity. Two dips then reach the level of the input squeezing component.

In conclusion, we investigate the quantum fluctuation spectra of the reflected field for the under-coupled, critically-coupled, and over-coupled optical cavity injected with squeezed vacuum state. The relationships between the quantum fluctuation reflected by the optical cavity and the type of coupling of the optical cavity are shown. The results indicate that the over-coupled optical cavity has obvious advantage in the manipulation of quantum fluctuation and can be used in the quan-

tum measurement and quantum information. This work well complements many previous studies based on bright quantum optical field[8−11,13] and gives a new perspective to understand the response of the cavity for the input quantum optical field. This work can also be applied to different systems, including the optical cavity[17−22] with input squeezed vacuum field.

References

1. A. E. Siegman, *Lasers* (University of Science Books, Sausalito, 1986).
2. R. W. P. Drever, J. L. Hall, F. V. Kowalski, J. Hough, and G. M. Ford, Appl. Phys. B **31,** 97 (1983).
3. G. C. Bjorklund, M. D. Levenson, W. Leath, and C. Ortiz, Appl. Phys. B **32,** 145 (1983)
4. E. D. Black, Am. J. Phys. **69,** 79 (2001).
5. B. J. J. Slagmolen, M. B. Gray, K. G. Baigent, and D. E. McClelland, Appl. Opt. **39,** 3638 (2000).
6. J. E. Heebner, V. Wong, A. Schweinsberg, R. W. Boyd, and D. J. Jackson, IEEE J. Quantum Electron. **40,** 726 (2004).
7. D. D. Smith and H. Chang, J. Mod. Opt. **51,** 2503 (2004).
8. M. D. Levenson, R. M. Shelby, and S. H. Perlmutter, Opt. Lett. **10,** 514 (1985).
9. P. Galatolaa, L. A. Lugiatob, M. G. Porrecac, P. Tombesic, and G. Leuchsd, Opt. Commun. **85,** 95 (1991).
10. J. Zhang, T. Zhang, K. Zhang, C. Xie, and K. Peng, J. Opt. Soc. Am. B **17,** 1920 (2000).
11. A. Zavatta, F. Marin, and G. Giacomelli, Phys. Rev. A **66,** 043805 (2002).
12. A. S. Villar, L. S. Cruz, K. N. Cassemiro, M. Martinelli, and P. Nussenzveig, Phys. Rev. Lett. **95,** 243603 (2005).
13. A. S. Villar, Am. J. Phys. **76,** 922 (2008).
14. G. S. Agarwal, Phys. Rev. Lett. **97,** 023601 (2006).
15. J. Zhang, C. Ye, F. Gao, and M. Xiao, Phys. Rev. Lett **101,** 233602 (2008).
16. K. Di, C. Xie, and J. Zhang, Phys. Rev. Lett. **106,** 153602 (2011).
17. A. C. Ji, X. C. Xie, and W. M. Liu, Phys. Rev. Lett. **99,** 183602 (2007).
18. Q. Liao, G. Fang, Y. Wang, M. A. Ahmad, and S. Liu, Chin. Opt. Lett. **8,** 1191 (2010).
19. A. C. Ji, Q. Sun, X. C. Xie, and W. M. Liu, Phys. Rev. Lett. **102,** 023602 (2009).
20. Q. Sun, X. H. Hu, W. M. Liu, X. C. Xie, and A. C. Ji, Phys. Rev. A **84,** 023822 (2011).
21. X. Yuan, K. Liu, W. Ye, and C. Zeng, Chin. Opt. Lett. **9,** 092301 (2011).
22. Q. Sun, X. H. Hu, A. C. Ji, and W. M. Liu, Phys. Rev. A **83,** 043606 (2011).